J. Braz. Chem. Soc., Vol. 5, No. 3, 131-135, 1994.
Printed in Brazil.

0103 – 5053 $5.00 + 0.00

The Temperature and Potential Dependences of the Oxygen Electroreduction Rate

*C.F. Zinola and A.M. Castro Luna**

Instituto de Investigaciones Fisicoquímicas Teóricas y Aplicadas (INIFTA), Universidad Nacional de La Plata, Sucursal 4, Casilla de Correo 16 (1900) La Plata, Argentina

Received: April 5, 1994; October 1, 1994

A cinética da reação de eletroredução de oxigênio (*RERO*) sobre eletrodos facetados dos tipos (111) e (100) foi estudada em H_2SO_4 1,0 M no intervalo de 8-62 °C. O coeficiente de Tafel na região de alta densidade de corrente sobre Pt facetada do tipo (111) aumenta com a temperatura aproximando-se da razão - 2,303 (2RT/F), enquanto que sobre Pt facetada do tipo (100) ele atinge um valor independente de temperatura igual a - 0,165 V/decada. A análise da dependência da velocidade da *RERO* com a temperatura e o potencial está baseada tanto nos efeitos de compensação entre a entalpia eletroquímica e a entropia de ativação como na influência do potencial sobre a energia livre de adsorção para os intermediários da *RERO*.

The kinetics of the oxygen electroreduction reaction *(OERR)* at faceted (111)- and (100)-type Pt electrodes was studied in 1.0 M H_2SO_4 in the 8-62 °C range. The Tafel slope in the high current density region on faceted (111)-type Pt increases with temperature, approaching the - 2.303 (2RT/F) ratio, whereas on faceted (100)-type Pt it reaches an independent temperature value equal to - 0.165 V/decade. The analysis of the temperature and potential dependences of the *OERR* rate is based on both the compensation effects between the electrochemical enthalpy and entropy of activation and the potential influence on the free energy of adsorption for the *OERR* intermediates.

Keywords: *oxygen, platinum, temperature, kinetic parameters*

Introduction

The *OERR* stationary kinetics on smooth polycrystalline (*pc*) and faceted Pt electrodes exhibits a Tafel slope in the *hcd* region, $(b_T)_{hcd}$, ranging from - 0.120 to - 0.165 V/decade, depending on the electrode topology and the surface coverage by *OERR* intermediates[1,2].

For the *OERR*, Yeager[3] and Appleby[4] found no significant changes of $(b_T)_{hcd}$ with temperature in concentrated H_3PO_4 in the 25-250 °C range. Conversely, Damjanovic *et al.*[5-7] report values of $(b_T)_{hcd}$ increasing with temperature in $HClO_4$ and H_2SO_4 down to 70 °C.

This work addresses the kinetics of the *OERR* in 1.0 M H_2SO_4 at different temperatures on faceted Pt surfaces. New results offer the possibility of obtaining thermodynamic data related to the activated process involved in the *OERR*.

Experimental

Faceted (111) and (100)-type Pt disks (99.999% purity, 3 mm of diameter) were prepared by the repetitive square wave potential program technique, as described elsewhere[8]. Electrochemical kinetic runs were made in aqueous O_2-free and O_2-saturated 1.0 M H_2SO_4 in the 8-62 °C range. A reversible hydrogen electrode (*RHE*) connected to the rest of the cell through a capillary tip was employed. A conventional thermostated two compartment cell, with the reference electrode compartment maintained at 25.0 °C, was used to perform the experiments at a constant potential (non-isothermal conditions)[9,10]. The kinetics of the *OERR* at different temperatures were followed by the rotating disk electrode (*RDE*) technique. Stationary polarization curves were obtained under potentiostatic conditions and displayed as Tafel plots after making the convective-diffusion contribution correction for a reaction order with respect to O_2 equal to 1. The values of the stationary Pt surface coverage by O-containing adsorbates, ϑ_T, were measured from the charge density, q_0, derived from the current transients recorded after applying a potential step from the preset potential down to 0.3 V, *i.e.* a potential value where the O-containing surface species are no longer

present. ϑ_T was calculated from the $q_0/2q_H$ ratio, q_H being the H-atom monolayer charge density on each faceted Pt surface[2].

All potentials in the text are referred to the *RHE* scale.

Results

The characterization of the Pt electrode surfaces was made by cyclic voltammetry in 1.0 M H_2SO_4 and *SEM* micrographs (Figs. 1 and 2, respectively). The *SEM* micrograph of faceted (111)-type Pt surfaces shows a random distribution of hexagonal Pt facets (Fig. 2a). Cyclic voltammetry of this Pt surface exhibits a large contribution of weakly bound H-atom adsorption sites in the hydrogen electrosorption region. The *SEM* micrograph of faceted (100)-type Pt is characterized by a large contribution of squared-pyramid shaped facets, as shown in Fig. 2b. In this case, the cyclic voltammetric profile run in the hydrogen electrosorption region shows a large contribution of strongly H-adatom reactive sites.

The reaction order with respect to O_2 was evaluated in a previous work[11] by log (I_D/I_K) *vs.* log (1-I_D/I_{LD}) plots in 1.0 M H_2SO_4 at different electrode potentials in the *hcd* region, I_K being the true kinetic *OERR* current, and I_{LD} the limiting current plateau. It was found that the reaction order was nearly 1, regardless of the type of faceted Pt surface. The number of electrons involved in the reaction was calculated from the Koutecky-Levich plots, resulting in 4 for the *OERR* at faceted (111)-type Pt and 3.8 at faceted (100)-type Pt[11, 12].

The presence of H_2O_2 in the course of the *OERR* was measured by the rotating ring-disk technique described in a previous work[2]. In the case of H_2SO_4 aqueous solutions the contribution of the peroxide pathway to the total kinetic current, when a parallel reaction mechanism is considered, gives negligible results (< 1 %) for faceted (111)-type Pt electrodes. For faceted (100)-type Pt the contribution of the peroxide path is slightly higher with respect to the former case[11].

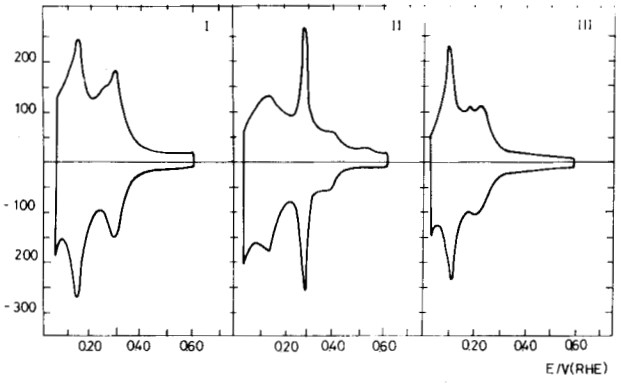

Figure 1. Cyclic voltammograms for *pc* (I), faceted (100)-type (II) and faceted (111)-type (III) Pt surfaces run at 0.1 V/s in 1.0 M H_2SO_4 at 25 °C.

Tafel plots for the *OERR* on faceted (111)- and (100)-type Pt in O_2-saturated 1.0 M H_2SO_4 at different temperatures are shown in Fig. 3. At the *hcd* region, the *OERR* on faceted (111)-type Pt exhibits $(b_T)_{hcd}$ values which increase with temperature, fitting the - 2.303 (2RT/F) ratio, whereas on faceted (100)-type Pt an almost temperature invariant value of $(b_T)_{hcd}$ = - 0.165 V/decade is obtained. At potentials higher than 0.93 V, Tafel lines approach a temperature independent - 0.060 V/decade slope for both faceted sur-

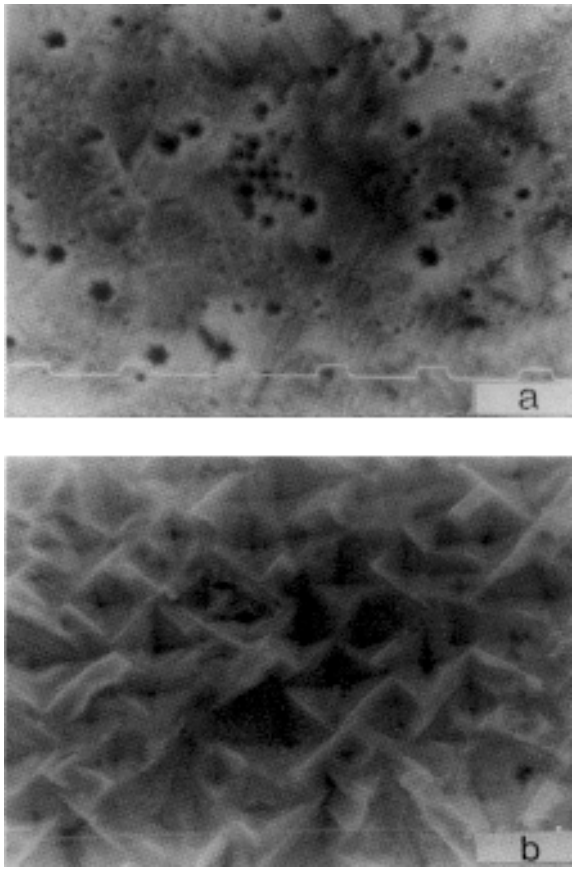

Figure 2. (a) SEM micrographs obtained for the faceted (111)-type Pt, scale 0.5 μm, and (b) for faceted (100)-type Pt, scale 1.3 μm.

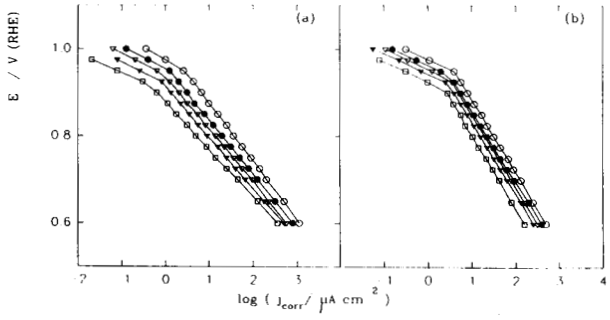

Figure 3. afel lines for *OERR* in O_2-saturated 1.0 M H_2SO_4 on (111)-type Pt and (100)-type Pt at different temperatures: (□) 8 °C, (▼)20 °C, (▽) 30 °C, (•) 40 °C, (o) 62 °C.

Table 1. *OERR* kinetic parameters for faceted (111)- and (100)-type Pt electrodes in O_2-saturated 1.0 M H_2SO_4 at 8, 20, 30, 40 and 62 °C.

T (°C)	$(b_T)_{hcd}$ (V/decate)	$(j_0)_{hcd}$ (A cm^{-2})
	(111) - type Pt	
8.0	0.111 ± 0.003	(5.6 ± 0.2) 10^{-10}
20.0	0.117 ± 0.003	(2.0 ± 0.2) 10^{-9}
30.0	0.119 ± 0.002	(3.9 ± 0.2) 10^{-9}
40.0	0.124 ± 0.002	(7.5 ± 0.2) 10^{-9}
62.0	0.135 ± 0.004	(2.3 ± 0.2) 10^{-8}
	(100) - type Pt	
8.0	0.166 ± 0.004	(3.9 ± 0.2) 10^{-8}
20.0	0.165 ± 0.004	(4.3 ± 0.2) 10^{-8}
30.0	0.164 ± 0.004	(5.0 ± 0.2) 10^{-8}
40.0	0.163 ± 0.004	(5.7 ± 0.2) 10^{-8}
62.0	0.162 ± 0.004	(7.6 ± 0.2) 10^{-8}

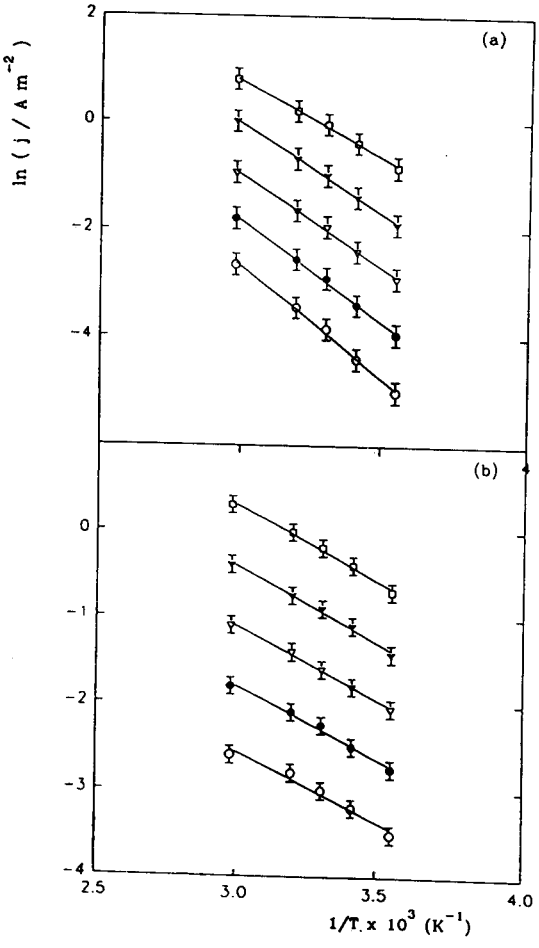

Figure 4. Arrhenius plots for the *OERR* in O_2-saturated 1.0 M H_2SO_4 on (111)-type Pt and (100)-type Pt for different E values: (o) 0.90 V, (•) 0.85 V, (▽) 0.80 V, (▼) 0.75 V, (□) 0.70 V.

faces as a result of the Pt oxide formation. Values of $(b_T)_{hcd}$ and $(j_0)_{hcd}$, the exchange current density in the *hcd* region for faceted (111)-type and (100)-type Pt at different temperatures, are presented in Table 1.

Electrochemical Arrhenius curves, ln j *vs.* 1/T, in the *hcd* region at different potentials are shown in Fig. 4. The electrochemical enthalpy of activation was obtained from the slope of these lines, and the logarithm of the pre-exponential factor, which contains the electrochemical entropy of activation, was derived from the intersection of Arrhenius lines with (1/T) = 0. For faceted (111)-type Pt, the electrochemical enthalpy of activation increases with the potential whereas for faceted (100)-type Pt it becomes almost constant. The pre-exponential factor, $(\ln j)_{1/T=0}$, also shows a different potential behavior for each type of faceted Pt electrode. For faceted (100)-type Pt, $(\ln j)_{1/T=0}$ changes with potential, whereas this dependence becomes negligible for faceted (111)-type Pt.

Discussion

Let us consider the influence of the potential on the chemical activation free energy, $\Delta G^{\#}$, for the *OERR*. It implies a change in the Fermi level of the electrons at the Pt surface, which is evidenced as a shift in $\Delta G^{\#}$ through αFE, α being the electrochemical transfer coefficient for the forward reaction. Thus, the electrochemical free energy of activation, $\Delta\tilde{G}^{\#}$, can be written as follows:

$$\Delta\tilde{G}^{\#} = \Delta G^{\#} + \alpha FE \qquad (1)$$

Earlier works[10], and references therein, have shown that the influence of the electrode potential on the reaction rate does not always correspond to a temperature independent α value. The potential influence on α can be better explained by a dual effect on both the electrochemical enthalpy and entropy of activation. Therefore, α is better expressed as $\alpha_H + \alpha_S T$, where α_H and α_S are the enthalpic and entropic contributions to α. Therefore, considering that $\Delta\tilde{G}^{\#} = \Delta\tilde{H} - T\Delta\tilde{S}^{\#}$,

$$\alpha_H = \frac{1}{F}\left(\frac{\partial\Delta\tilde{H}^{\#}}{\partial E}\right)_T \qquad \alpha_S = \frac{1}{F}\left(\frac{\partial\Delta\tilde{S}^{\#}}{\partial E}\right)_T \qquad (2a, b)$$

As a consequence of the catalytic behavior of the *OERR*, changes in the activation barriers due to adsorption should be considered. The influence of the adsorption of species in a chemical reaction was first considered by Brönsted[13], extended to electrochemical systems by Horiuti and Polanyi[14] and re-examined by Appleby[15].

For an electrocatalytic reaction such as the *OERR*, the value of the activation barrier is modified by the presence of intermediate adsorbates. The effective electrochemical free energy of activation, $\Delta\tilde{G}^{\#}_{eff}$, is lower than $\Delta\tilde{G}^{\#}$ (without adsorption), and is determined by considering the stabilization of the *rds* product through $\Delta\tilde{G}_{ad}$ that is, it is due to a

decrease in the ground-state energy of the *OERR* products in the *rds*. The contribution of product adsorption to the activation barrier is reflected in the *OERR* current density expression by an exponential term of $\gamma\Delta\tilde{G}_{ad}$. γ is a geometrical factor arising from linearized Morse plots, which considers the variation in the jump distance for the electron transfer to the particles as a consequence of product adsorption.

Among the different proposed mechanisms for the *OERR*, an alternative two-step pathway consistent with our experimental results is suggested, as follows:

$$O_2 + Pt + H^+ + e^- \xrightarrow{rds} [(O_2H)Pt]_{ad} \quad (I)$$

$$[(O_2H)Pt]_{ad} + H^+ + e^- \Rightarrow \text{products} \quad (II)$$

As such, the overall rate of the *OERR* in the *hcd* region can be expressed in terms of the current density of step (I), j_I:

$$j_I = \kappa F(kT/h)c_{H^+}\, kP_{O_2}(1 - \vartheta_T) \exp(-\Delta\tilde{G}^{\#}/RT) \exp(\gamma\Delta\tilde{G}_{ad}/RT) \quad (3)$$

where κ is the nuclear transmission coefficient for reactants, k is the Henry constant for O_2, c_{H^+} is the H^+ ion concentration in the bulk of the solution, and P_{O_2} is the O_2 saturation pressure.

Since the adsorption process changes $\Delta\tilde{G}^{\#}$ through $\Delta\tilde{G}_{ad}$, the knowledge of ϑ_T as a function of the potential is required for each faceted Pt surface. On both Pt surfaces, ϑ_T linearly depends on the potential as follows:

$$\vartheta_T = \vartheta_{E=0} + \mathbf{K}E \quad (4)$$

where $\mathbf{K} \equiv (\partial\vartheta_T / \partial E)$ at a constant temperature, and $\vartheta_{E=0}$ is the hypothetical fractional Pt surface coverage by O-intermediates obtained at E = 0 V. **K** is a parameter that depends on the Pt electrode surface, resulting in 0.85 V^{-1} and 4.25 V^{-1} for faceted (111)-type and (100)-type Pt, respectively[2].

Experimental data for ϑ_T fits a Temkin isotherm, leading to a potential dependence of $\Delta\tilde{G}_{ad}$:

$$\Delta\tilde{G}_{ad} = \Delta G_{ad,\vartheta_{T=0}} + r\vartheta_{E=0} + r\mathbf{K}E \quad (5)$$

where $r = (\partial\Delta\tilde{G}_{ad}/\partial\vartheta_T)$ at a constant temperature, and $\Delta G_{ad,\vartheta_{T=0}}$ is the free energy of adsorption at zero surface coverage. Since $\Delta G_{ad,\vartheta_{T=0}}$ includes the work function of metal, Φ^{Pt}, and it depends on the crystallography of the electrode, a crystal orientation dependence for $\Delta G_{ad,\vartheta_{T=0}}$ arises from the adsorption of intermediates. For Pt single crystals, Φ^{Pt} is 6.22 eV on Pt(111) and 5.80 eV on Pt(100)[16], resulting in larger values of $\Delta G_{ad,\vartheta_{T=0}}$ for the *OERR* intermediates on Pt(100).

Taking into account Eq. 5, the *OERR* currrent density, is given, by:

$$j_I = \kappa F(kT/h)c_{H^+}\, kP_{O_2}(1-\vartheta_T) \exp(-\Delta\tilde{G}^{\#}/RT) \exp[(\gamma\Delta\tilde{G}_{ad,\vartheta_{T=0}} + \gamma r\vartheta_{E=0} + \gamma r\mathbf{K}E)/RT] \quad (6)$$

On the other hand, considering the enthalpic and entropic components of $\Delta\tilde{G}^{\#}$ through Eqs. 2a, b, and neglecting the potential dependence of the pre-exponential term, a simplified *OERR* current density results:

$$j_I = K \exp(-\alpha_H FE/RT) \exp(\alpha_S FE/R) \exp(\gamma r\mathbf{K}E/RT) \quad (7)$$

From Eq. 7, the expression for $(b_T)_{hcd}$ is:

$$(b_T)_{hcd} = -\frac{2.303\ RT}{[\alpha_H - T\,\alpha_S - \gamma r\mathbf{K}/F]\,F} \quad (8)$$

In order to evaluate the temperature dependence of $(b_T)_{hcd}$, Arrhenius plots were treated to calculate the potential dependences of both the effective electrochemical enthalpy and entropy of activation $\Delta\tilde{H}^{\#}_{eff}$ and $\Delta\tilde{S}^{\#}_{eff}$.

Since, the theoretical expression for $\Delta\tilde{H}^{\#}_{eff}$ is:

$$\Delta\tilde{H}^{\#}_{eff} = \Delta H^{\#} - \gamma\Delta H_{ad,\vartheta_{T=0}} - \gamma r\vartheta_{E=0} + [-\gamma r\mathbf{K} + \alpha_H F]\,E \quad (9)$$

and for faceted (100)-type Pt, the potential coefficient of $\Delta\tilde{H}^{\#}_{eff}$, $(\partial\Delta\tilde{H}^{\#}_{eff}/\partial E)$, is - 5.1 kJ mol^{-1} V^{-1}, therefore: $[\alpha_H - \gamma r\mathbf{K}/F] = -0.052$.

On the other hand, the expression for $\Delta\tilde{S}^{\#}_{eff}$, obtained from the Arrhenius pre-exponential factor, is:

$$\Delta\tilde{S}^{\#}_{eff} = \Delta S^{\#} + \gamma\Delta S_{ad,\vartheta_{T=0}} + \alpha_S FE \quad (10)$$

As such, considering the potential dependence of $(\ln j)_{1/T=0}$ for faceted (100)-type Pt, $\alpha_S = -1.2\ 10^{-3}\ K^{-1}$. For instance, at 303 K, $\alpha_S T = -0.37$, so that the entropic contribution to α is greater than $(\alpha_H - \gamma r\mathbf{K}/F)$. The simplified expression for $(b_T)_{hcd}$ is thereby independent of temperature, and given by the following equation:

$$(b_T)_{hcd} = -2.303\ R/\alpha_S F \quad (11)$$

Hence, for the *OERR* on faceted (100)-type Pt, the Tafel slope for the *hcd* lead to a temperature independent value of - 0.163 V/decade, in agreement with the experimental data at all temperatures (Table 1).

For faceted (111)-type Pt, ϑ_T values are lower than 0.2 in the *hcd* region, so $\Delta\tilde{G}_{ad}$ can be considered almost constant and equal to $\Delta\tilde{G}_{ad\,\vartheta_{T=0}}$. Accordingly, the potential contribution of $\Delta\tilde{G}_{ad}$ to the overall current density becomes negligible, that is a langmuirian behavior. In this case, the potential dependence of $\Delta\tilde{H}^{\#}_{eff}$ yields a slope equal to $\alpha_H F$. Taking into account that the experimental potential coefficient of $\Delta\tilde{H}^{\#}_{eff}$ is 50 kJ mol^{-1} V^{-1}, $\alpha_H = 0.5$ is obtained. In addition, $(\ln j)_{1/T=0}$ is independent of potential, so it will lead to negligible α_S values. From the

data of Fig. 4, the slope of the $(\ln j)_{1/T=0}$ *vs.* E plot results in $\alpha_S \sim 10^{-6}\ K^{-1}$.

Since $\alpha_H = 0.5$ and $\alpha_S \sim 10^{-6}\ K^{-1}$, the current density for the *OERR* on faceted (111)-type Pt results in the following expression for $(b_T)_{hcd}$:

$$(b_T)_{hcd} = -2.303\ RT/\alpha_H F \qquad (12)$$

Equation 12 shows that $(b_T)_{hcd}$ becomes temperature dependent, for instance, at T = 298 K, $(b_T)_{hcd}$ = - 0.118 V/decade. This behavior agrees with the simplified classical electrode kinetics found on this type of Pt electrode.

Conclusions

1) A reaction scheme was proposed to interpret kinetic data of the *OERR* temperature dependence on faceted Pt electrodes in acid solution with a *rds* involving adsorbed species, which are responsible for the decrease in the activation barrier.

2) A Temkin adsorption isotherm was considered for the *OERR* adsorbed intermediates at faceted (100)-type Pt. Greater ϑ_T and $(\partial\vartheta_T/\partial E)$ values caused a large potential dependence of $\Delta\tilde{G}_{ad}$ at this surface.

3) The influence of the potential on $\Delta\tilde{H}^{\#}$ and $\Delta\tilde{S}^{\#}$, which leads to the expression $\alpha = \alpha_H + \alpha_S T$, was considered. α_S is the major factor responsible for the temperature independence of $(b_T)_{hcd}$ on faceted (100)-type Pt, whereas for faceted (111)-type Pt, as α_S has a negligible value, a temperature dependent $(b_T)_{hcd}$ results.

Acknowledgments

This work was financially supported by the Consejo Nacional de Investigaciones Científicas y Técnicas *(CONICET)* of Argentina. C.F.Z. thanks the Universidad de la República, Montevideo (Uruguay), for a fellowship. A.M.C.L. is a member of the Research Career of the Comision de Investigaciones de la Provincia de Buenos Aires *(CIC)*.

References

1. F. Kadiri, R. Faure and R. Durand, *J. Electroanal. Chem.* **301**, 1 (1991).
2. C.F. Zinola, A.M. Castro Luna, W.E. Triaca and A.J. Arvia, *J. Appl. Electrochem.* **24**, 119 (1994).
3. J.C. Huang, R.K. Sen and E. Yeager, *J. Electrochem. Soc.* **26**, 786 (1988).
4. A.J. Appleby, *J. Electrochem. Soc.* **117**, 328 (1970).
5. D.B. Sepa, M.V. Vojnovic, Lj.M. Vracar and A. Damjanovic, *Electrochim. Acta.* **31**, 91 (1986); and *ibid* **31**, 97 (1986).
6. D.B. Sepa, M.V. Vojnovic, Lj.M. Vracar and A. Damjanovic, *Electrochim. Acta* **31**, 1105 (1986).
7. A. Damjanovic and D.B. Sepa, *Electrochim. Acta* **35**, 1157 (1990).
8. W.E. Triaca, T. Kessler, J.C. Canullo and A.J. Arvia, *J. Electrochem. Soc.* **134**, 1165 (1987).
9. J.N. Agar, *Discuss. Faraday Soc.* **1**, 81 (1947).
10. B. Conway, *Modern Aspects of Electrochemistry* (B. Conway, J.O'M. Bockris and R. White, eds., Plenum Press, N.Y., 1985), vol. 16.
11. C.F. Zinola, A.M. Castro Luna, W.E. Triaca and A.J. Arvia, *Electrochim. Acta* **39**, 1627, special issue devoted to the *Ferrara Symposium in Electrocatalysis: Theory and Practice* (1994).
12. C.F. Zinola, A.M. Castro Luna, W.E. Triaca and A. J. Arvia, *J. Appl. Electrochem.* **24**, 531 (1994).
13. J.N. Bronsted, *Chem. Rev.* **5**, 231 (1928).
14. J. Horiuti and M. Polanyi, *Acta Physicochim. URSS* **2**, 505 (1935).
15. A.J. Appleby, *Comprehensive Treatise of Electrochemistry* (B. Conway, J.O'M. Bockris, E. Yeager, S. Khan and R. White, eds., Plenum Press, New York - London, 1983), vol. 6.
16. S. Trasatti, *Comprehensive Treatise of Electrochemistry* (J.O'M. Bockris, B. Conway and E. Yeager, eds., Plenum Press, New York, 1980), vol. 1.